ISSN 1068-1620, Russian Journal of Bioorganic Chemistry, 2021, Vol. 47, No. 1, pp. 158–165. © Pleiades Publishing, Ltd., 2021.

Synthesis, Molecular Docking, In Silico ADME Predictions, and Toxicity Studies of *N*-Substituted-5-(4-Chloroquinolin-2-yl)-1,3,4-Thiadiazol-2-Amine Derivatives as COVID-19 Inhibitors

Hanaa S. Mohamed[a], Walaa S. El-Serwy[a, 1], and Weam S. El-Serwy[b]

[a] *Department of Therapeutic Chemistry, Pharmaceutical and Drug Industries Research Division, National Research Centre, Dokki, Giza, 12622 Egypt*

[b] *Chemistry of Natural and Microbial Products Department, Pharmaceutical and Drug Industries Research Division, National Research Centre, Dokki, Giza, 12622 Egypt*

Received August 28, 2020; revised September 10, 2020; accepted September 12, 2020

Abstract—The present study aimed to synthesis *N*-substituted-5-(4-chloroquinolin-2-yl)-1,3,4-thiadiazol-2-amine derivatives. Molecular docking study of the synthesized compounds was carried out. COVID-19 docked with the synthesized compounds and the results indicated that the binding energies of docking 6LU7 with native ligand, and the synthesized compounds were −8.1, −8.0, −7.7, −7.5, −7.4, −7.3, −7.2, −6.7, −6.6, −6.5, and −5.4 kcal/mol.

Keywords: COVID-2019, *N*-substituted-5-(4-chloroquinolin-2-yl)-1,3,4-thiadiazol-2-amine derivatives

DOI: 10.1134/S1068162021010155

INTRODUCTION

Coronaviruses are found to be responsible for different infections in humans [1]. New kind of this virus was appearing in Wuhan, China at the end of 2019 [2]. On the other hand, in the market most of the today's drugs are heterocyclic compounds, quinoline among these heterocycles is an important one. The quinoline ring has diverse activities, such as antimicrobial [3], anti-inflammatory [4], antituberculosis [5], antimalarial [6], antihypertensive [7], antibiotic [8], antiHIV [9] and tyrokinase PDGF-RTK inhibiting agents [10]. Also, 1,3,4-thiadiazole is a nitrogen containing compounds show a broad spectrum of pharmacological activities [11–15]. We synthesized *N*-substituted-5-(4-chloroquinolin-2-yl)-1,3,4-thiadiazol-2-amine derivatives in order to investigate their biological activities, but as a result of the significant disruption that is being caused by the COVID-19 pandemic we couldn't study their biological activities in laboratory so we calculated it theoretically.

Prompted by this, in the present study we investigated *N*-substituted-5-(4-chloroquinolin-2-yl)-1,3,4-thiadiazol-2-amine derivatives as potential inhibitor candidates for COVID-19 with the help of molecular docking studies and the two heterocyclic moieties are combined together to enhance their activities. In this study, we have measured the interaction of COVID-19 main protease in complex with an inhibitor N3 (PDB ID 6LU7) with *N*-substituted-5-(4-chloroquinolin-2-yl)-1,3,4-thiadiazol-2-amine derivatives.

[1] Corresponding author: e-mail: walaasalah16@yahoo.com.

RESULTS AND DISCUSSION

Chemistry

4-Chloro-2-[2-substituted-amino-1,3,4-thiadiazole-5-yl]quinoline (**IIa–i**) produced by the reaction of 4-hydroxyquinaldic acid (**I**) and the appropriate thiosemicarbazides (Scheme 1). IR of compound (**IIa**) showed bands at 3330, 3300 cm^{-1} confirming to the (NH_2). Moreover, IR spectrum of compounds (**IIb**), (**IIc**) and (**IId**) showed absorption band ν_{max} = 3150, 3125 and 3110 cm^{-1} refers to the (NH), respectively. ^1H NMR (DMSO-d_6) of compound (**IIa**) showed signals at δ 5.50 ppm, representing NH_2 group which exchangeable by D_2O, on the other hand, ^1H NMR (DMSO-d_6) spectra of compound (**IIb**) revealed signals at δ 1.22 and 3.44 ppm, representing CH_3 and CH_2 groups of the ethyl group, respectively. Also, ^1H NMR (DMSO-d_6) spectra of compound (**IIc**) revealed signals at δ 6.15 and 6.95 ppm representing CH_2 and NH groups, respectively. ^1H NMR (DMSO-d_6) spectra of compound (**IId**) revealed signals at δ 4.5 ppm representing NH group.

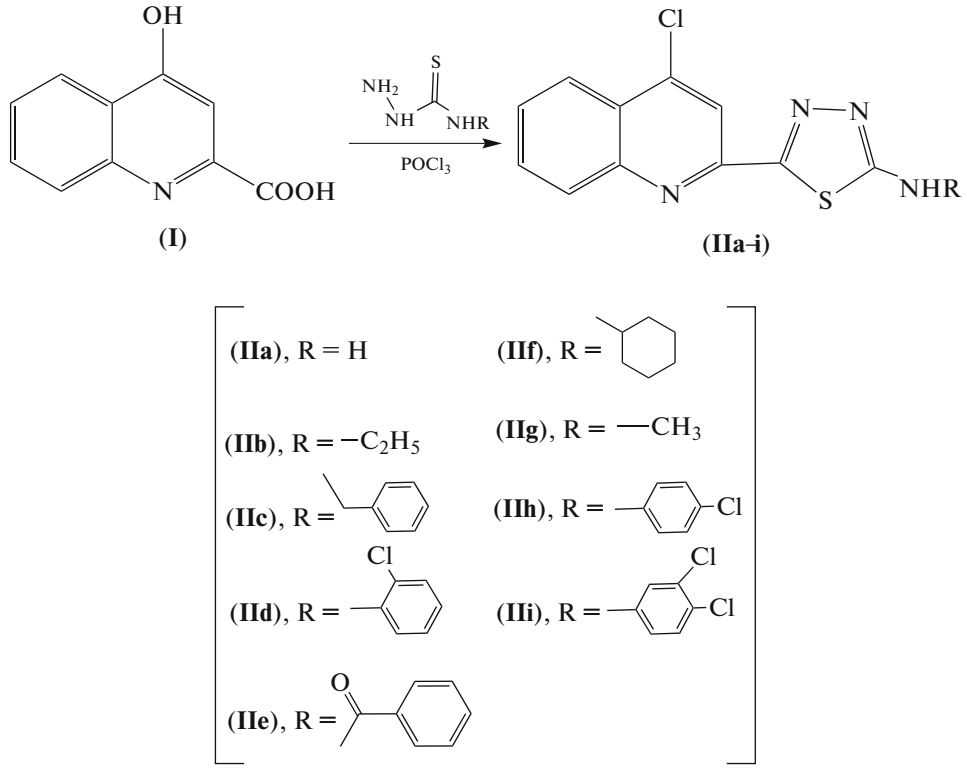

Scheme 1. Synthetic routes of 4-chloro-2-[2-substituted-amino-1,3,4-thiadiazole-5-yl]quinoline derivatives (**IIa–i**).

Molecular Docking

Molecular docking studies of *N*-substituted-5-(4-chloroquinolin-2-yl)-1,3,4 thiadiazol-2-amine derivatives were carried out and the docking scores of these compounds are in the range of −8.0 to −5.4 kcal/mol (Table 1 and Fig. 1). From the results it showed that compound (**I**) forms 4 hydrogen bonds with GLU166, LEU141, CYS145 and GLY143 (Figs. 2a, 3a) (see Supplementary Information). Compound (**IIa**) forms 3 hydrogen bonds with GLU166, LEU141 and HIS163 (Figs. 2b, 3b) (see Supplementary Information). Moreover, compound (**IIb**) forms 3 hydrogen bonds with SER144, SER144 and CYS145 (Figs. 2c, 3c) (see Supplementary Information). Also, compound (**IIc**) forms 3 hydrogen bonds with SER144, HIS163 and LEU141 (Figs. 2d, 3d) (see Supplementary Informa-

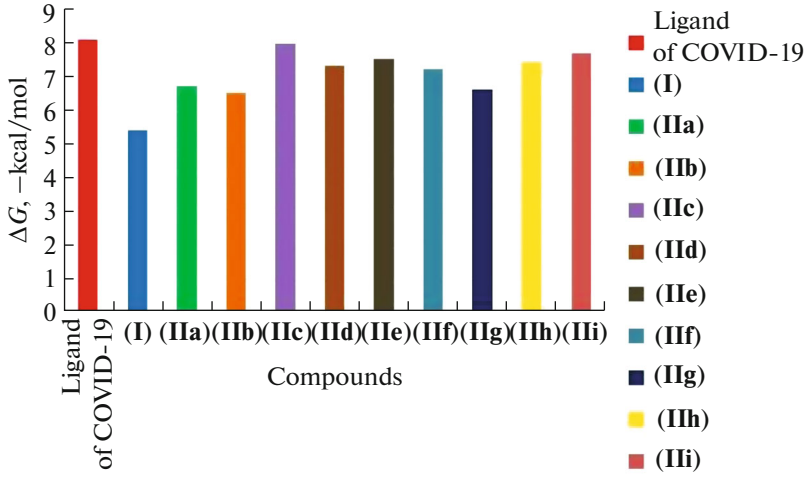

Fig. 1. Histogram showing molecular docking results between 6LU7 and compounds (**I**) and (**IIa–i**).

Table 1. The protein-ligand interactions of native ligand of COVID-19, (**I**) and (**IIa–i**) with active site pocket 6LU7

Ligand	Binding energy	Amino acids involved in the interaction	Length of hydrogen bonds
Native ligand of COVID-19	−8.1	ASN142	H-bond acceptor 2.41 Å
		GLN189	H-bond acceptor 2.08 Å
		GLN189	H-bond acceptor 1.95 Å
		GLN189	H-bond acceptor 2.79 Å
		GLU166	H-bond acceptor 2.12 Å
		SER144	H-bond acceptor 2.58 Å
		CYS145	H-bond acceptor 2.29 Å
(I)	−5.4	GLU166	H-bond acceptor 2.34 Å
		LEU141	H-bond acceptor 2.27 Å
		CYS145	H-bond acceptor 2.60 Å
		GLY143	H-bond acceptor 2.28 Å
(IIa)	−6.7	GLU166	H-bond acceptor 2.74 Å
		LEU141	H-bond acceptor 2.36 Å
		HIS163	H-bond acceptor 2.73 Å
(IIb)	−6.5	SER144	H-bond acceptor 2.08 Å
		SER144	H-bond acceptor 2.50 Å
		CYS145	H-bond acceptor 2.57 Å
(IIc)	−8.0	SER144	H-bond acceptor 2.22 Å
		HIS163	H-bond acceptor 2.63 Å
		LEU141	H-bond acceptor 3.09 Å
(IId)	−7.3	CYS145	H-bond acceptor 2.46 Å
		SER144	H-bond acceptor 2.29 Å
		LEU141	H-bond acceptor 3.10 Å
(IIe)	−7.5	CYS145	H-bond acceptor 2.38 Å
		SER144	H-bond acceptor 2.01 Å
		HIS163	H-bond acceptor 2.31 Å
(IIf)	−7.2	SER144	H-bond acceptor 2.19 Å
		SER144	H-bond acceptor 2.50 Å
		CYS145	H-bond acceptor 2.55 Å
		HIS163	H-bond acceptor 2.60 Å
(IIg)	−6.6	SER144	H-bond acceptor 1.97 Å
		CYS145	H-bond acceptor 2.35 Å
		HIS163	H-bond acceptor 2.19 Å
(IIh)	−7.4	GLU166	H-bond acceptor 2.12 Å
		HIS164	H-bond acceptor 2.47 Å
(IIi)	7.7	GLU166	H-bond acceptor 2.03 Å
		HIS164	H-bond acceptor 2.55 Å

tion). In addition, compound (**IId**) forms 3 hydrogen bonds with CYS145, SER144 and LEU141 (Figs. 2e, 3e) (see Supplementary Information). On the other hand, compounds (**IIe**) and (**IIg**) form 3 hydrogen bonds with CYS145, SER144 and HIS163 (Figs. 2f, 3f) (Figs. 2h, 3h) (see Supplementary Information), respectively. Compound (**IIf**) forms 4 hydrogen bonds with SER144, SER144, CYS145 and HIS163 (Figs. 2g, 3g) (see Supplementary Information). Compounds (**IIh**) and (**IIi**) form 2 hydrogen bonds with GLU166 and HIS164 (Figs. 2i, 3i) (Figs. 2j, 3j) (see Supplementary Information), respectively.

Physicochemical and ADME Parameters

Compounds (**I**) and (**IIa–i**) were evaluated for ADME properties in using SwissADME web tool [16]. The oral bioavailability chart of all the compounds shown in (Fig. 4) (see Supplementary Information). BOILED-Egg in SwissADME web tool is also used [17], all compounds were in the white region except compound (**I**) (Fig. 5) (see Supplementary Information). The synthesized compounds (**I**) and (**IIa–i**) complies well with the Lipinski's rule with a violation no more than one (Table 2). Literature implies that TPSA < 140 is essential for good absorption. The

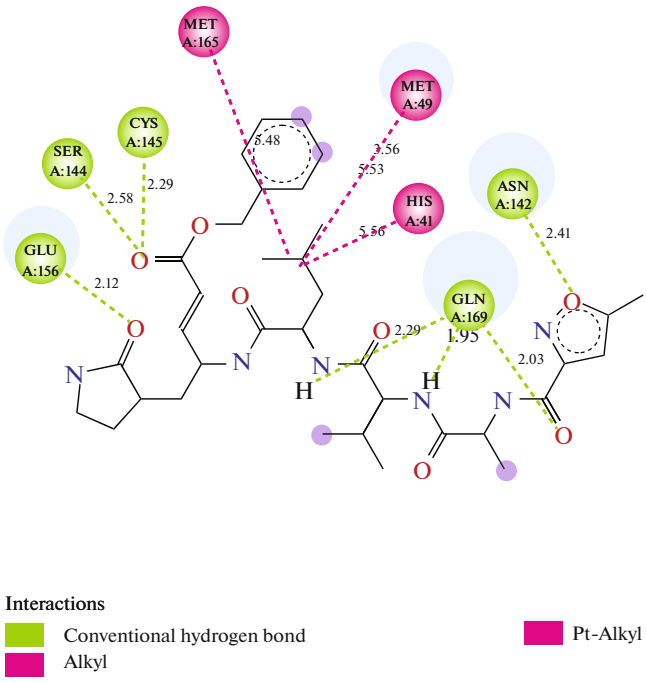

Fig. 2. Active site of the target enzyme.

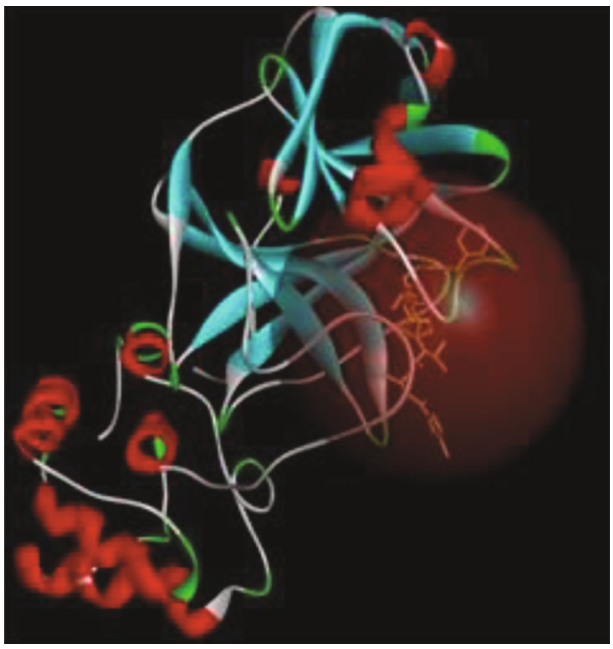

Fig. 3. High-resolution crystal structure of a novel coronavirus target (PDB 6LU7). The circle in the figure is the position of the active pocket.

acceptable region for suitable absorption for all the synthesized compounds is between 70.42 and 96.01 Å^2. All of the compounds exhibited high GIT absorption and no BBB permeability except compounds No. **(I)** and **(IIg)**.

In Silico Toxicity Predictions

We employed the web-servers ProTox-II to predict the toxicity parameters. From Table 3 it revealed that compounds **(IIb)** and **(IIc)** are inactive on (hepatotoxicity) and (carcinogenicity, immunotoxicity, mutagenicity, and cytotoxicity). On the other hand, compound **(IIa)** is active on (hepatotoxicity) and (carcinogenicity and mutagenicity).

Structure-Activity Relationship

The structure-activity relationship proved that the addition of 1,3,4-thiadiazol ring to the quinoline ring resulted in a significant increase in the binding efficiency with 6LU7, which is evident from the binding energy values of the starting compound **(I)** and all other prepared compounds **(IIa–IIi)**, it also improved

Table 2. Physicochemical property profile of compounds **(I)** and **(IIa–i)** calculated by SwissADME web tool

Compound	[a]TPSA Å^2	[b]log P	[c]BBB permeant	[d]GI absorption	Bio availability score	[e]*n*-HBD	[f]*n*-HBA	[g]Lipinski
(I)	70.42	1.07	Yes	High	0.56	2	4	Yes (0)
(IIa)	92.93	2.12	No	High	0.55	1	3	Yes (0)
(IIb)	78.94	3.01	No	High	0.55	1	3	Yes (0)
(IIc)	78.94	3.28	No	High	0.55	1	3	Yes (0)
(IId)	78.94	3.59	No	High	0.55	1	3	Yes (0)
(IIe)	96.01	2.70	No	High	0.55	1	4	Yes (0)
(IIf)	78.94	3.29	No	High	0.55	1	3	Yes (0)
(IIg)	78.94	2.65	Yes	High	0.55	1	3	Yes (0)
(IIh)	78.94	3.44	No	High	0.55	1	3	Yes (0)
(IIi)	78.94	3.54	No	High	0.55	1	3	Yes (1)

ADME (absorption, distribution, metabolism, and excretion), [a]Topological polar surface area; [b]log of the partition coefficient (P); [c]BBB, blood-brain barrier; [d]GI, Gastrointestinal absorption; [e]*n*-HBD: number of hydrogen bond donors; [f]*n*-HBA: number of hydrogen bond acceptors; [g]Lipinski violation Rule of 5.

Table 3. Predicted toxicities for compounds **(I)** and **(IIa–i)**

Compounds	Hepatotoxicity	Carcinogenicity	Immunotoxicity	Mutagenicity	Cytotoxicity
(I)	Y (0.51)	N (0.66)	N (0.92)	N (0.95)	N (0.78)
(IIa)	Y (0.68)	Y (0.50)	N (0.98)	Y (0.58)	N (0.73)
(IIb)	N (0.56)	N (0.56)	N (0.91)	N (0.54)	N (0.57)
(IIc)	N (0.54)	N (0.58)	N (0.96)	N (0.54)	N (0.55)
(IId)	Y (0.67)	N (0.60)	N (0.95)	Y (0.50)	N (0.81)
(IIe)	Y (0.67)	N (0.52)	N (0.99)	N (0.53)	N (0.80)
(IIf)	Y (0.50)	N (0.58)	N (0.93)	Y (0.50)	N (0.73)
(IIg)	Y (0.65)	N (0.58)	N (0.99)	Y (0.55)	N (0.74)
(IIh)	Y (0.68)	N (0.59)	N (0.95)	Y (0.53)	N (0.76)
(IIi)	Y (0.67)	N (0.60)	N (0.92)	Y (0.50)	N (0.81)

(Probability): Y (Yes, active) or N (No, inactive).

Activity color Key	Color
Active	
Inactive	

their physicochemical and bioavailability properties. Furthermore, analysis of the docking data revealed that substitution at amine of thiadiazol moiety with benzyl group in compound **(IIc)** is responsible for the good binding efficiency with 6LU7, also responsible for making the compound inactive on organ toxicity (hepatotoxicity) and toxicity endpoints (carcinogenicity, immunotoxicity, mutagenicity, cytotoxicity). On the other hand, substitution at amine of thiadiazol moiety with 2-chlorophenyl group in compound **(IIb)** is responsible for decrease binding efficiency with 6LU7.

EXPERIMENTAL

Chemistry

All materials, reagents and solvents were purchased from Sigma-Aldrich, Merck and Fisher chemicals. Elemental microanalyses were carried out at Micro analytical Unit. ^{1}H spectra were recorded at 298 K on a JEOL ECA-500 spectrometer (^{1}H at 500.16 MHz), and were processed using the Bruker Topspin 3.2 software. ^{1}H spectra are referenced to ^{1}H signals of residual non-deuterated solvents. ^{1}H NMR signals are reported with chemical shift values δ (ppm), multiplicity (s = singlet, d = doublet, t = triplet, q = quartet, m = multiplet and br = broad. Mass spectra were recorded on a JEOL DART+ HI RESOLUTION mass spectrometer and ionization of all samples was carried out using ESI. Analytical TLC was performed on Merck silica gel 60 F254 pre-coated aluminum plates (0.2 mm) and visualized under UV light (254 nm).

4-Chloro-2-[2-substituted amino-1,3,4-thiadiazole-5-yl]quinoline (IIa–i). To a mixture of 4-hydroxyquinaldic acid **(I)** (0.002 mol), (0.002 mol) of the appropriate thiosemicarbazides and (16 mL) phosphorus oxychloride was added drop wise while shaking at 10–15°C. The reaction mixture was refluxed for 1–3 h and excess phosphorous oxychloride were driven off under vacuo. The residue was then poured onto ice-water and the formed solid was filtered off, washed with water, air dried and finally recrystallized from DMF/EtOH to give the title compounds.

5-(4-Chloroquinolin-2-yl)-1,3,4-thiadiazol-2-amine (IIa). Yield 90%. IR (KBr) ν, cm^{-1}: 3330, 3300 (NH_2). ^{1}H NMR (DMSO-d_6, δ, ppm): 5.50 (2H, s, NH_2, D_2O exchangeable), 7.26–8.30 (5H, m, Ar–H). MS *m/z*: M^+ 262 (5%), M^{+2}. 264 (3%). Anal. calcd. for

$C_{11}H_7ClN_4S$ (262.72): C, 50.29; H, 2.69; N, 21.33. Found: C, 50.02; H, 2.49; N, 21.48. (lit. compound (**IIe**). Yield 70%. IR (KBr) ν, cm^{-1}: 3150 (NH), 1680 (C=O). ^1H NMR (DMSO-d_6, δ, ppm): 7.3–8.7 (10H, m, Ar–H), 11.0 (1H, s, NH, D_2O exchangeable). MS *m/z*: M^+ 366 (0.47%). Anal. calcd. for $C_{18}H_{11}ClN_4OS$ (366.90): C, 58.90; H, 3.03; N, 15.27. Found: C, 59.05; H, 3.13; N, 15.30. [18]), (lit. compound (**IIf**). Yield 75%. IR (KBr) ν, cm^{-1}: 3300 (NH). ^1H NMR (DMSO-d_6, δ, ppm): 1.39 (s, 2H, CH_2), 1.60 (s, 2H, CH_2), 1.70 (s, 2H, CH_2), 2.50 (d, 2H, CH_2), 2.96 (d, 2H, CH_2), 7.6–8.3 (5H, m, Ar–H), 10.20 (1H, s, NH, D_2O exchangeable). MS *m/z*: M^+ 344 (70%). Anal. calcd. for $C_{17}H_{17}ClN_4S$ (344.95): C, 59.19; H, 4.98; N, 16.25. Found: C, 59.29; H, 5.10; N, 16.37. [18]), (lit. compound (**IIg**). Yield 71%. MS *m/z*: M^+ 276 (100%). Anal. calcd. for $C_{12}H_9ClN_4S$ (276.86): C, 52.06; H, 3.28; N, 20.24. Found: C, 52.08; H, 3.31; N, 20.26. [18]), (lit. compound (**IIh**). Yield 66%. MS *m/z*: M^+ 372 (54%). Anal. calcd. for $C_{17}H_{10}Cl_2N_4S$ (372.38): C, 54.68; H, 2.71; N, 15.01. Found: C, 54.70; H, 2.73; N, 15.07. [18]), (lit. compound (**IIi**). Yield 70%. MS *m/z*: M^+ 406 (4%). Anal. calcd. for $C_{17}H_9Cl_3N_4S$ (407.87): C, 50.06; H, 2.23; N, 13.74. Found: C, 50.08; H, 2.33; N, 13.87. [18]).

5-(4-Chloroquinolin-2-yl)-N-ethyl-1,3,4-thiadiazol-2-amine (IIb). Yield 70%. IR (KBr) ν, cm^{-1}: 3150 (NH). ^1H NMR (DMSO-d_6, δ, ppm): 1.22 (3H, t, CH_3 of ethyl), 3.44 (2H, q, CH_2 of ethyl), 7.79–7.94 (5H, m, Ar–H), 8.10 (1H, t, NH, D_2O exchangeable). MS *m/z*: M^+ 290 (40%), M^{+2}. 292 (10%). Anal. calcd. for $C_{13}H_{11}ClN_4S$ (290.77): C, 53.70; H, 3.81; N, 19.27. Found: C, 53.82; H, 3.70; N, 19.39. (lit. compound (**IIe**). Yield 70%. IR (KBr) ν, cm^{-1}: 3150 (NH), 1680 (C=O). ^1H NMR (DMSO-d_6, δ, ppm): 7.3–8.7 (10H, m, Ar–H), 11.0 (1H, s, NH, D_2O exchangeable). MS *m/z*: M^+ 366 (0.47%). Anal. calcd. for $C_{18}H_{11}ClN_4OS$ (366.90): C, 58.90; H, 3.03; N, 15.27. Found: C, 59.05; H, 3.13; N, 15.30. [18]), (lit. compound (**IIf**). Yield 75%. IR (KBr) ν, cm^{-1}: 3300 (NH). ^1H NMR (DMSO-d_6, δ, ppm): 1.39 (s, 2H, CH_2), 1.60 (s, 2H, CH_2), 1.70 (s, 2H, CH_2), 2.50 (d, 2H, CH_2), 2.96 (d, 2H, CH_2), 7.6–8.3 (5H, m, Ar–H), 10.20 (1H, s, NH, D_2O exchangeable). MS *m/z*: M^+ 344 (70%). Anal. calcd. for $C_{17}H_{17}ClN_4S$ (344.95): C, 59.19; H, 4.98; N, 16.25. Found: C, 59.29; H, 5.10; N, 16.37. [18]), (lit. compound (**IIg**). Yield 71%. MS *m/z*: M^+ 276 (100%). Anal. calcd. for $C_{12}H_9ClN_4S$ (276.86): C, 52.06; H, 3.28; N, 20.24. Found: C, 52.08; H, 3.31; N, 20.26. [18]), (lit. compound (**IIh**). Yield 66%. MS *m/z*: M^+ 372 (54%). Anal. calcd. for $C_{17}H_{10}Cl_2N_4S$ (372.38): C, 54.68; H, 2.71; N, 15.01. Found: C, 54.70; H, 2.73; N, 15.07. [18]), (lit. compound (**IIi**). Yield 70%. MS *m/z*: M^+ 406 (4%). Anal. calcd. for $C_{17}H_9Cl_3N_4S$ (407.87): C, 50.06; H, 2.23; N, 13.74. Found: C, 50.08; H, 2.33; N, 13.87. [18]).

***N*-Benzyl-5-(4-chloroquinolin-2-yl)-1,3,4-thiadiazol-2-amine (IIc)**. Yield 85%. IR (KBr) ν, cm^{-1}: 3125 (NH). ^1H NMR (DMSO-d_6, δ, ppm): 6.15 (2H, s, CH_2), 6.95 (1H, t, NH, D_2O exchangeable), 7.07–8.21 (10H, m, Ar–H). MS *m/z*: M^+ 352 (10%), M^{+2}. 354 (6%). Anal. calcd. for $C_{18}H_{13}ClN_4S$ (352.84): C, 61.27; H, 3.71; N, 15.88. Found: C, 61.37; H, 3.60; N, 15.95. (lit. compound (**IIe**). Yield 70%. IR (KBr) ν, cm^{-1}: 3150 (NH), 1680 (C=O). ^1H NMR (DMSO-d_6, δ, ppm): 7.3–8.7 (10H, m, Ar–H), 11.0 (1H, s, NH, D_2O exchangeable). MS *m/z*: M^+ 366 (0.47%). Anal. calcd. for $C_{18}H_{11}ClN_4OS$ (366.90): C, 58.90; H, 3.03; N, 15.27. Found: C, 59.05; H, 3.13; N, 15.30. [18]), (lit. compound (**IIf**). Yield 75%. IR (KBr) ν, cm^{-1}: 3300 (NH). ^1H NMR (DMSO-d_6, δ, ppm): 1.39 (s, 2H, CH_2), 1.60 (s, 2H, CH_2), 1.70 (s, 2H, CH_2), 2.50 (d, 2H, CH_2), 2.96 (d, 2H, CH_2), 7.6–8.3 (5H, m, Ar–H), 10.20 (1H, s, NH, D_2O exchangeable). MS *m/z*: M^+ 344 (70%). Anal. calcd. for $C_{17}H_{17}ClN_4S$ (344.95): C, 59.19; H, 4.98; N, 16.25. Found: C, 59.29; H, 5.10; N, 16.37. [18]), (lit. compound (**IIg**). Yield 71%. MS *m/z*: M^+ 276 (100%). Anal. calcd. for $C_{12}H_9ClN_4S$ (276.86): C, 52.06; H, 3.28; N, 20.24. Found: C, 52.08; H, 3.31; N, 20.26. [18]), (lit. compound (**IIh**). Yield 66%. MS *m/z*: M^+ 372 (54%). Anal. calcd. for $C_{17}H_{10}Cl_2N_4S$ (372.38): C, 54.68; H, 2.71; N, 15.01. Found: C, 54.70; H, 2.73; N, 15.07. [18]), (lit. compound (**IIi**). Yield 70%. MS *m/z*: M^+ 406 (4%). Anal. calcd. for $C_{17}H_9Cl_3N_4S$ (407.87): C, 50.06; H, 2.23; N, 13.74. Found: C, 50.08; H, 2.33; N, 13.87. [18]).

***N*-(2-Chlorophenyl)-5-(4-chloroquinolin-2-yl)-1,3,4-thiadiazol-2-amine (IId)**. Yield 90%. IR (KBr) ν, cm^{-1}: 3110 (NH). ^1H NMR (DMSO-d_6, δ, ppm): 4.50 (1H, s, NH, D_2O exchangeable), 7.12–8.33 (9H, m, Ar–H). MS *m/z*: M^+ 373 (100%), M^{+2}. 375 (70%). Anal. calcd. for $C_{17}H_{10}Cl_2N_4S$ (373.26): C, 54.70; H, 2.70; N, 15.01. Found: C, 54.85; H, 2.84; N, 14.91. (lit. compound (**IIe**). Yield 70%. IR (KBr) ν, cm^{-1}: 3150 (NH), 1680 (C=O). ^1H NMR (DMSO-d_6, δ, ppm): 7.3–8.7 (10H, m, Ar–H), 11.0 (1H, s, NH, D_2O exchangeable). MS *m/z*: M^+ 366 (0.47%). Anal. calcd. for $C_{18}H_{11}ClN_4OS$ (366.90): C, 58.90; H, 3.03; N, 15.27. Found: C, 59.05; H, 3.13; N, 15.30. [18]), (lit. compound (**IIf**). Yield 75%. IR (KBr) ν, cm^{-1}: 3300 (NH). ^1H NMR (DMSO-d_6, δ, ppm): 1.39 (s, 2H, CH_2), 1.60 (s, 2H, CH_2), 1.70 (s, 2H, CH_2), 2.50 (d, 2H, CH_2), 2.96 (d, 2H, CH_2), 7.6–8.3 (5H, m, Ar–H), 10.20 (1H, s, NH, D_2O exchangeable). MS *m/z*: M^+ 344 (70%). Anal. calcd. for $C_{17}H_{17}ClN_4S$ (344.95): C, 59.19; H, 4.98; N, 16.25. Found: C, 59.29; H, 5.10; N, 16.37. [18]), (lit. compound (**IIg**). Yield 71%. MS *m/z*: M^+ 276 (100%). Anal. calcd. for $C_{12}H_9ClN_4S$ (276.86):

C, 52.06; H, 3.28; N, 20.24. Found: C, 52.08; H, 3.31; N, 20.26. [18]), (lit. compound (**IIh**). Yield 66%. MS *m/z*: M^+ 372 (54%). Anal. calcd. for $C_{17}H_{10}Cl_2N_4S$ (372.38): C, 54.68; H, 2.71; N, 15.01. Found: C, 54.70; H, 2.73; N, 15.07. [18]), (lit. compound (**IIi**). Yield 70%. MS *m/z*: M^+ 406 (4%). Anal. calcd. for $C_{17}H_9Cl_3N_4S$ (407.87): C, 50.06; H, 2.23; N, 13.74. Found: C, 50.08; H, 2.33; N, 13.87. [18])

Molecular Docking

Protein–ligand docking studies of the synthesized derivatives (**I**) and (**IIa–i**) were evaluated to investigate the interaction between the active site of 6LU7 enzyme and the synthesized derivatives (**I**) and (**IIa–i**) on Hp computer system, with Intel (R) Core (TM) i5-4200M CPU @2.50 GHz 2.50 GHz, 6 GB of RAM using AutoDock Vina 1.5.6 screening software, and Biovia Discovery Studio software.

Preparation of the Protein

6LU7 is the main protease (Mpro) found in COVID-19, which been structured and repositioned in PDB and can be accessed by the public, as of early February 2020. The 6LU7 protein contains two chains, A and B, which form a homodimer. Chain A was used for macromolecule preparation, and the inhibitor N3 was removed. The ligand N3 (*N*-[(5-methylisoxazol-3yl)carbonyl]alanyl-l-valyl-*n*~1~-((1*R*,2*Z*)-4-(benzyloxy)-4-oxo-1-{[(3*R*)-2-oxopyrrolidin-3-yl]methyl}but-2-enyl)-l-leucinamide) was used as a control.

The crystal structure of the molecular target, enzyme COVID-19 (PDB ID: 6LU7), was retrieved from RCSB protein data bank (https://www.rcsb.org/) [19]. Target needs to be prepared before starting the molecular docking process, which involves removal of the water molecules and native ligand attached with target and other heteroatoms which may provide hindrance in the simulation. Besides, hydrogen atoms were added into a target. These processes were carried out in the AutoDock Vina 1.5.6 [20] window execution file. Docking protocol was first validated by re-docking of the original ligand of 6LU7 in the vicinity of the active site of the protein forming a docking pose with an energy score (S) = –8.1 kcal/mol. The active site of this target enzyme is composed of ASN142, GLN189, GLN189, GLN189, GLU166, SER144, and CYS145 (Fig. 6). The corresponding "active pocket" was constructed and system searched for the "active pocket" near the active site, and finally, –10.711837, 12.411388, and 68.831286 were defined as an active pocket (Fig. 7).

Preparation of the Ligand

Compounds were built in ChemDraw Ultra version 15.0 and their energy minimized through Chem3D Ultra version 11.0/MM2, Jop Type: minimum RMS Gradient of 0.100. The investigation ligand was loaded and their torsions along with rotatable bonds are assigned and the files are saved as ligand.PDBQT. In the current study, identification of binding modes of the synthesized derivatives with the target was identified using AutoDock Vina 1.5.6 software program. Moreover, to confirm actual binding interaction with targets, blind docking was performed and the best conformers were represented with lowest binding energy (–kcal/mol) which might have the way to disclose the mode of actions of these ligands. The ligand and protein molecules were converted to their proper readable file format (pdbqt) using AutoDock Vina tools 1.5.6. The docking was done using an exhaustiveness value of 8. All other parameters of software were kept as default and all bonds contained in ligand were allowed to rotate freely, considering receptor as rigid. The final visualization of the docked structure was performed using Discovery Studio Visualizer.

SwissADME Prediction Tool

SwissADME is a reliable free online tool [21] that predicts the physicochemical properties of the compounds. The bioavailability and pharmacokinetic parameters of any synthetic compound are obtained by inputting its structure on the website. http://www.swissadme.ch/index.php.

In Silico Toxicity Predictions

We employed the web-servers ProTox-II (http://tox.charite.de/protox_II/) [22] to predict the toxicity parameters.

CONCLUSION

In this study, *N*-substituted-5-(4-chloroquinolin-2-yl)-1,3,4-thiadiazol-2-amine derivatives were synthesized. Molecular docking and prediction of ADMET properties of compounds was carried out, respectively. The results indicated that compounds (**IIc**, **IIi**, **IIe**, **IIh**, **IId**, and **IIf**) can act as COVID-19 inhibitor.

COMPLIANCE WITH ETHICAL STANDARDS

Experiments does not contain any studies with humans/animals.

Conflict of Interests

No conflict of interest is there to declare.

SUPPLEMENTARY INFORMATION

The online version contains supplementary material available at 10.1134/S1068162021010155.

REFERENCES

1. Malik, Y.S., Sircar, Sh., Bhat, S., Sharun, Kh., Dhama, K., Dadar, M., Tiwari, R., and Chaicump, W., *Vet. Q*, 2020, vol. 40, pp. 1–12. https://doi.org/10.1080/01652176.2020.1727993
2. Lee, P.I. and Hsueh, P.R., *J. Microbiol. Immunol. Infect.*, 2020, vol. 53, pp. 365–367. https://doi.org/10.1016/j.jmii.2020.02.001
3. Eswaran, S., Adhikari, A.V., and Shetty, N.S., *Eur. J. Med. Chem.*, 2009, vol. 44, pp. 4637–4647. https://doi.org/10.1016/j.ejmech.2009.06.031
4. Leatham, P.A., Bird, H.A., Wright, V., Seymour, D., and Gordon, A., *Eur. J. Rheumatol. Inflamm.*, 1983, vol. 6, pp. 209–211.
5. Lilienkampf, A., Jialin, M., Baojie, W., Yuehong, W., Franzblau, S.G., and Kozikowski, A.P., *J. Med. Chem.*, 2009, vol. 52, pp. 2109–2118.
6. Nasveld, P. and Kitchener, S., *Trans. R. Soc. Trop. Med. Hyg.*, 2005, vol. 99, pp. 2–5. https://doi.org/10.1016/j.trstmh.2004.01.013
7. Muruganantham, N., Sivakumar, R., Anbalagan, N., Gunasekaran, V., and Leonard, J.T., *Biol. Pharm. Bull.*, 2004, vol. 27, pp. 1683–1687. https://doi.org/10.1248/bpb.27.1683
8. Mahamoud, A., Chevalier, J., Davin-Regli, A., Barbe, J., and Pages, J.M., *Curr. Drug Targets*, 2006, vol. 7, pp. 843–847. https://doi.org/10.2174/138945006777709557
9. Strekowski, L., Honkan, V.A., Czarny, A., Cegla, M.T., Wydra, R.L., Patterson, S.E., Mokrosz, J.L., and Schinazi, R.F., *J. Med. Chem.*, 1991, vol. 34, pp. 1739–1746. https://doi.org/10.1021/jm00109a031
10. Maguire, M.P., Sheets, K.R., McVety, K., Spada, A.P., and Zilberstein, A., *J. Med. Chem.*, 1994, vol. 37, pp. 2129–2137. https://doi.org/10.1021/jm00040a003
11. Padmavathi, V., Nagi, R.S., and Mahesh, K., *Chem. Pharm. Bull.*, 2009, vol. 57, pp. 1376–1380. https://doi.org/10.1248/cpb.57.1376
12. Salimon, J., Salih, N., Hameed, A., Ibraheem, H., and Yousif, E., *J. Appl. Sci. Res.*, 2010, vol. 6, pp. 866–870. https://doi.org/10.13140/rg.2.2.29127.55203
13. Mishra, P., Jatav, V., Jain, S., and Kashaw, S., *Indian J. Pharm. Sci.*, 2006, vol. 68, pp. 360–363. https://doi.org/10.4103/0250-474x.26679
14. Zamani, K., Faghihi, K., Tofighi, T., and Shariatzadeh, M.R., *Turk. J. Chem.*, 2004, vol. 28, pp. 95–100.
15. Schenone, S., Brullo, C., Bruno, O., Bondavalli, F., Ranise, A., Filippelli, W., Rinaldi, B., Capuano, A., and Falcone, G., *Bioorg. Med. Chem.*, 2006, vol. 14, pp. 1698–1705. https://doi.org/10.1016/j.bmc.2005.10.064
16. www.swissadme.ch/index.php.
17. Daina, A. and Zoete, V., *Chem. Med. Chem.*, 2016, vol. 11, pp. 1117–1121.
18. Kassem, E.M.M., *Egypt. J. Chem.*, 1999, vol. 42, pp. 413–419.
19. Berman, H.M., Battistuz, T., Bhat, T.N., Bluhm, W.F., Bourne, Ph.E., Burkhardt, K., Feng, Z., Gilliland, G.L., Iype, L., Jain, Sh., Fagan, Ph., Marvin, J., Padilla, D., Ravichandran, V., Schneider, B., Thanki, N., Weissig, H., Westbrook, J.D., and Zardecki, Ch., *Acta. Crystallogr. Sect. D. Biol. Crystallogr.*, 2002, vol. 58, pp. 899–907.
20. Trott, O. and Olson, A.J., *J. Comput. Chem.*, 2010, vol. 31, pp. 455–461.
21. Daina, A., Michielin, O., and Zoete, V., *Sci. Rep.*, vol. 7, pp. 1–13.
22. Banerjee, P., Eckert, A.O., Schrey, A.K., and Preissner, R., *Nucleic Acids Res.*, 2018, vol. 46, pp. W257–W263.